

# Of Diamonds, Rings, and Bracelets: Local Values of the Response Parameter can Increase the Synchronization Probability in Pulse-Coupled Oscillators

Arke Vogell, Udo Schilcher, Jorge F. Schmidt, and Christian Bettstetter  
*Institute of Networked and Embedded Systems, University of Klagenfurt, Austria*  
email: arke.vogell@aau.at

**Abstract**—Not all systems of pulse-coupled oscillators converge to synchrony from any initial configuration. The probability of synchronization depends on the network topology and the phase response function. It is often assumed that all oscillators are governed by the same phase response function. We exemplify that the synchronization probability can be significantly increased by using node-individual (local) values for the phase response parameter — rather than a single, global value. This insight motivates research into algorithms for parameter adjustment in self-organized network synchronization.

**Index Terms**—pulse-coupled oscillators, synchronization, self-organization, emergence

## 1. Introduction

Synchronization occurs frequently in nature and is a crucial feature in many engineered systems when distributed entities must act in a coordinated manner — e.g., in communications and computing, transport, and energy. Synchrony can be a desired or undesired system state: Fireflies flash in synchrony to attract mates [1], heart pacemaker cells synchronize to control the contraction of muscles [2], and desynchronization in electrical power grids can lead to serious outages [3]. Synchronized movements of pedestrians could pose a hazard to structures [4], synchrony of Internet routers can lead to long-term congestion [5], and synchronization of neurons is associated with Parkinson's disease [6].

Many synchronization phenomena can be modeled with pulse-coupled oscillators (PCOs). Each oscillator is a periodic system that follows an internal cycle. At one point in this cycle, the oscillator emits a pulse. Other oscillators receiving such a pulse adjust their internal cycle by changing the oscillation frequency or phase (the current position on the cycle). This interaction may bring the pulses of two or more oscillators into alignment—they synchronize in a distributed and self-adaptive way. Such a technique is preferred over centralized ones if the network is dynamic and single points of failure should be avoided.

A group of all-to-all coupled PCOs that advance their phase by a fixed value on each pulse reception synchronize for almost all initial conditions [7]. Conditions for this proof of convergence can be relaxed, e.g., by utilizing different response functions [8], [9], [10], considering delays [11], [12], and using other network topologies [13], [14], [15],

[16]. The cited papers include proofs of convergence under specific conditions. Other papers have shown that synchrony is guaranteed when the phases of all oscillators are close enough [17], [18] and that non-synchronizing states do exist [13], [19]. Whether or not an arbitrary network of PCOs synchronizes remains an open question.

The author team recently studied a phenomenon that prevents synchronization in a network of PCOs [20]. This raised the question of how probable it is that a system initialized with random phases eventually synchronizes. That question was answered for a network with an underlying star topology. The work at hand studies the synchronization probability for other types of undirected networks, which contain one or more cycles (in contrast to the cycle-free star graph). As in [20], we use a piecewise linear, delay-advance phase response function (prf) whose slope is controlled by a response parameter  $a$ . Our goal is to determine the probability of synchronization  $\mathcal{P}$  starting from a random point in the state space and study the impact of adjusting  $a$  on  $\mathcal{P}$ . The overall objective of our research activities in this domain is to obtain an understanding of the fundamental question: Is it beneficial to use node-individual  $a$ -values rather than a single network-wide  $a$ -value as commonly done? The answer would motivate techniques in which this parameter is selected (and maybe adjusted) locally on each oscillator. This paper is a first step in this direction.

Our contributions are threefold: First, we discuss the possible non-synchronizing states and conditions favoring their occurrence. Second, we propose to use the phase response function—specifically its parameter  $a$ —as a potential “screw” to make randomly initialized systems more likely to synchronize. This proposition is motivated by numerical findings on the synchronization probability for three types of graphs. Third, we show that local adjustment of the response parameter can further boost the synchronization probability for these graphs. The findings give insights and serve as motivation for a distributed algorithm to determine the best  $a$  for each node. A corresponding algorithm is subject of future work.

The rest of the paper is structured as follows: Section 2 defines the PCO model used. Section 3 introduces the types of states that prevent synchronization. Sections 4 and 5 study how the phase response parameter affects the synchronization probability  $\mathcal{P}$ , both as a global and a local parameter. Section 6 concludes the paper.

## 2. Coupling model

An oscillator is a one-dimensional periodic system with a phase  $\theta$  ranging from zero to one, which increases with a constant speed of  $\dot{\theta} = 1$ . On reaching one, the phase is reset to zero and the oscillator emits a pulse. This is called firing event. In a network of multiple oscillators, pulses are transmitted instantaneously to all neighbors. An oscillator's reaction to a received pulse is given by the phase response function (prf), here given by

$$h_a(\theta) = \begin{cases} (1-a)\theta & \text{for } \theta \leq 0.5 \\ a + (1-a)\theta & \text{for } \theta > 0.5. \end{cases} \quad (1)$$

A pulse that is received while  $\theta \leq 0.5$  reduces the receiving oscillator's phase towards 0 (inhibitory coupling), whereas a pulse received while  $\theta > 0.5$  increases it towards 1 (excitatory coupling). The response parameter  $a \in [0, 1]$  determines how large the change in phase is. In the literature, this type of prf is called delay-advance prf (or type-II prf due to its relation to the response function of class-II neurons [8]).

## 3. Non-synchronizing states

The described PCO system will end up in one of three states: it will either reach (i) a synchronized state, in which all oscillators reach the firing threshold at the same time indefinitely, (ii) a locked state, in which the timings of all oscillators' pulse events lock onto a (non-synchronized) periodic pattern, or (iii) run into a deadlock state, in which at least one of the oscillators is prevented from sending a pulse (as described in [20]). The occurrence of deadlocks is usually associated with a locked state in the remaining (potentially unconnected) network.

Theoretically, the period of locked states can be much longer than the typical time between two firing events. Empirically, however, we have observed that the vast majority of locked states in the networks studied has a period similar to that of an individual oscillator.

Deadlock states can occur due to the inhibitory effect from a received pulse. If a sufficient number of such pulses is received frequently enough, the receiving oscillator may never reach the firing threshold. In this situation, the receiving oscillator is in a deadlock. Any locked state in which one or more oscillators are in a deadlock is called a deadlock state. We know that deadlock states presuppose at least one oscillator with enough links to be prevented from firing [20]. The number of required links for a deadlock and its likelihood are closely tied to the response parameter  $a$ .

Another mechanism that prevents synchronization is an onset of chaos [21], [22]. The emergence of chaos is commonly tied to specific setups and interactions [23] or external signals [19], [22], [21]. Whereas noise is indeed present in communication and computer systems, its effect on the communication between nodes differs from that of external signals in the above references. Additionally, we only consider networks of identical oscillators that do not distinguish between pulses from different neighbors, which

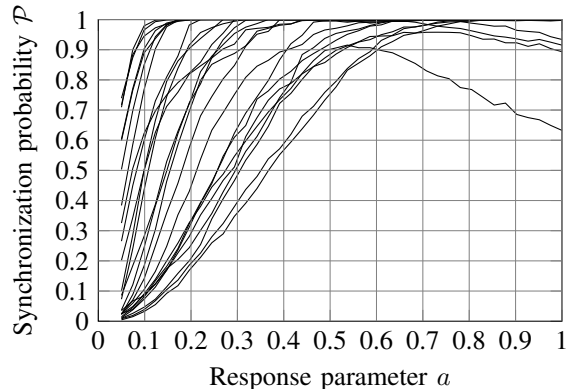


Figure 1. Synchronization probability  $\mathcal{P}$  for connected Erdős-Rényi graphs of pulse-coupled oscillators over the (global) response parameter  $a$ . Each curve represents a different graph. The overall trend of the synchronization probability is similar among all graph realizations, however, for a few it decreases again for large  $a$ . This figure is adapted from [20], where we also discuss the occurrence of deadlock states being responsible for some curves not converging to  $\mathcal{P} = 1$ .

is paramount for the results in [23]. We therefore assume that chaos will not play a major role in the following discussion.

In previous work on non-synchronizing states [20], we observed the following for random graphs (see Fig. 1): Locked states occur more often for small than for medium to large  $a$ . Most random graphs synchronize almost certainly for sufficiently large  $a$ , but some curves clearly show a maximum in  $\mathcal{P}$  for certain  $a < 1$  and then decrease with  $a \rightarrow 1$ . From the same work, we know that increasing  $a$  beyond a critical value potentially introduces the probability of a system running into a deadlock. The possibility of deadlocks appearing (for large  $a$ ) and the critical value depend on the underlying topology.

Likewise, the probability  $\mathcal{P}$  depends on the topology, as it is the only difference between the systems simulated for Fig. 1. To gain more insight of what specific aspects of topology are relevant for this dependence, we now consider two specific building blocks of networks (rings and diamonds) and then combine them to a new type of topology (which we call diamond bracelet).

## 4. Synchronization probability

The synchronization probability  $\mathcal{P}$  for a network of  $n$  oscillators is the relative volume of the configuration space ( $C_n = [0, 1]^n \subset \mathbb{R}^n$ ) for which the system converges to a synchronized state (i.e.,  $S_n \subset C_n$ , s.t.  $s \in S_n$  converges to a synchronized state):  $\mathcal{P} = \text{vol}(S_n) / \text{vol}(C_n)$ . Convergence to a synchronized state is guaranteed if at any time all phases lie within a closed interval in the phase domain (i.e.,  $\mathbb{R}/1$ ) of diameter one half [17]. We estimate  $\mathcal{P}$  through a Monte-Carlo simulation which is terminated on reaching the convergence guarantee or detecting a periodic state.

We now study  $\mathcal{P}$  as a function of  $a$  for three types of undirected, connected graphs (shown in Fig. 2) to find how different topologies affect  $\mathcal{P}$ . We know from [13] that

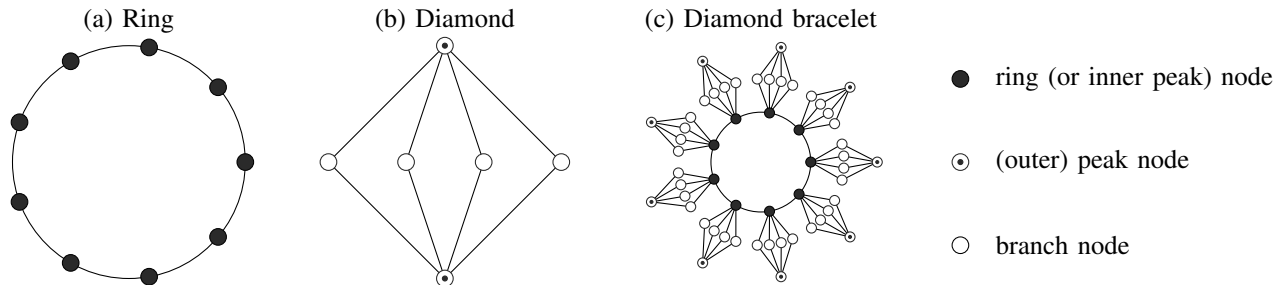


Figure 2. The three graph types under study: ring (with  $n_R = 9$ ), diamond (with  $n_B = 4$ ), and diamond bracelet (with  $n_R = 9$  and  $n_B = 4$ ).

ring graphs (Fig. 2 (a)) support a multitude of locked states. Their number increases with the number of ring nodes  $n_R$ . However, as every node has a degree of two, no deadlocks are attainable [20]. Because loops in a graph seem to promote the existence of locked states and high-degree nodes allow for deadlocks, we consider a variant of the diamond graph as our second investigated topology (Fig. 2 (b)). It has two high-degree peak nodes and  $n_B$  branch nodes that form several loops. With every added branch node, we incorporate more loops and increase the degree of the peak nodes while keeping the loop size constant. As a third topology, we combine ring and diamond (Fig. 2 (c)) by adding an  $n_B$ -diamond to every node of a ring of size  $n_R$  (i.e., we identify each ring node with a peak node of one of  $n_R$  diamonds with  $n_B$  branch nodes, linking these diamonds at the selected peak nodes to form a ring). We call this topology an  $(n_R, n_B)$ -diamond bracelet.

For each of these topologies, we are interested in the maximum achievable synchronization probability  $\mathcal{P}$  and the corresponding value of the response parameter  $a$  for which this maximum is achieved. Reaching synchrony is a commonly sought goal in networked computing and communication systems. Exploiting the optimal  $a$  that provides the best chance of achieving synchrony in a given network (whose initial configuration cannot be controlled) is thus relevant for the implementation of such systems.

#### 4.1. Ring

A ring is a connected graph with  $n_R \geq 3$  nodes in which each node is linked to exactly two other nodes. An example is shown in Fig. 2 (a). Rings of PCOs allow for locked states, which can be identified by symmetry operations [13]. The larger  $n$ , the more potential locked states exist. There are no synchronization deadlocks in rings because it takes at least three neighbors to keep an oscillator in a deadlock.

We numerically study  $\mathcal{P}$  as a function of  $a$  for five ring sizes  $n_R$  (see results in Fig. 3). Two basic observations can be made: First, the choice of  $a$  has a strong impact on  $\mathcal{P}$ ; the probability monotonically rises to one for increasing  $a$ . Second, larger rings have a lower synchronization probability.

The locked states in rings form different patterns based on  $n_R$ ,  $a$ , and the initial configuration. The possible patterns are described in [12]. We most commonly observed *wave*

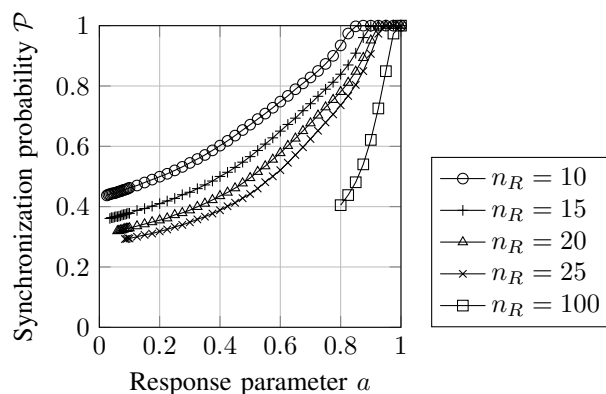


Figure 3. Synchronization probability  $\mathcal{P}$  for rings. A ring of  $n_R$  PCOs (almost) always synchronizes for a response parameter  $a = 1$ . Smaller values of  $a$  sometimes converge to a locked state, where the probability for such state happening from a random initial configuration increases with decreasing  $a$ .

patterns with different wavelengths. Other patterns are also possible but seem to occur less frequently.

Like random graphs, for small  $a$ , rings seem to converge to locked states more often. Unlike random graphs, however, they are incapable of exhibiting deadlocks. We next study a graph that is capable of both.

#### 4.2. Diamond

An  $n_B$ -diamond graph is an undirected graph of two peak nodes and  $n_B$  branch nodes, where all branch nodes are connected to both peak nodes. No other link exists in the graph. An example is visualized in Fig. 2 (b). A diamond with  $n_B = 2$  is identical to a four-node ring. The  $n_B$ -diamond (with  $n_B > 2$ ) can exhibit both deadlock states (for large  $a$ ) and locked states (for small  $a$ ).

Figure 4 shows  $\mathcal{P}$  as a function of  $a$ . Non-synchronizing states exist for small and large  $a$ ; the maximum synchronization probability is in between. All graphs tested show a maximum  $\mathcal{P}$  close to one, but the response parameter for this maximum depends on  $n_B$ . For large  $a$ , the reduced synchronization probability is due to deadlocks at the peak nodes; for small  $a$ , it is caused by locked states. Locked states in the low (but not the lowest)  $a$  regime ( $0.1 \lesssim a \lesssim 0.4$ ) occur

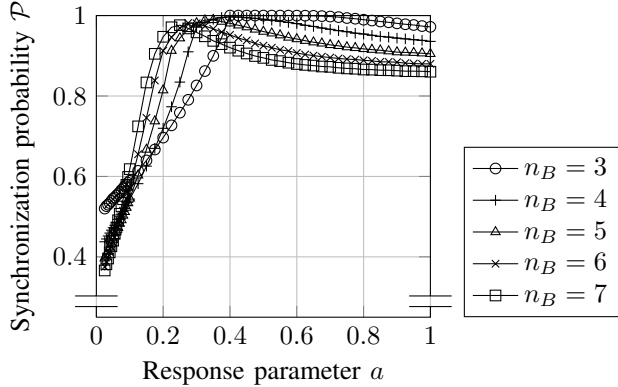


Figure 4. Synchronization probability  $\mathcal{P}$  for diamonds. Very small  $a$  allow for locked states, like in rings. As opposed to rings we observe deadlocks for large  $a$ . The deadlock probability increases with  $n_B$ . Values are based on 500,000 simulations using random (uniformly drawn) initial phases.

more often for diamonds with fewer branch nodes. For very low  $a \lesssim 0.1$ , the opposite is true, however, our simulations suggest that  $\mathcal{P}$  is similar for all  $n_B > 3$  in that regime. In the high  $a$  regime,  $n_B$ -diamonds may exhibit deadlocks and  $\mathcal{P}$  is lower for higher  $n_B$ . This corresponds to our results on star graphs, where the probability for the central node suffering from a deadlock is higher if the number of neighbors is larger [20].

We continue with a third graph that combines and amplifies the tendencies observed. So far we have seen that larger loops (in rings) and fewer loops (in diamonds) increase the probability for locked states when  $a$  tends to zero. Furthermore, nodes with a high degree are prone to deadlocks for large  $a$ . We now construct a graph that allows for one parameter ( $n_R$ ) to increase an underlying loop and another ( $n_B$ ) to increase the degree of certain nodes.

### 4.3. Diamond bracelet

An  $(n_R, n_B)$ -diamond bracelet consists of a ring with  $n_R$  nodes and as many  $n_B$ -diamonds. The diamonds are joined with the ring at one of their peak nodes, forming a ring of  $n_B$ -diamonds. We distinguish between three types of nodes based on their role in the graph structure: *ring nodes* are the peak nodes in the diamonds at which they are connected to other diamonds (inner peak nodes), *branch nodes* describe all the branch nodes in all diamonds, and *outer peak nodes* refer to the diamonds' peak nodes that are not connected to other diamonds. An example is visualized in Fig. 2 (c). This graph contains a large loop of diameter  $n_R/2$  and  $n_R$  nodes with degree  $n_B + 2$ , the maximum degree in the graph. Like the  $n_B$ -diamond, this graph exhibits both locked states and deadlocks.

The simulation results in Fig. 5 show the following: First, the synchronization probability in diamond bracelets for large  $a$  is significantly lower than in the single diamond. This is to be expected because a deadlock in any of the  $n_R$  diamonds prevents synchronization. Second, the maximum

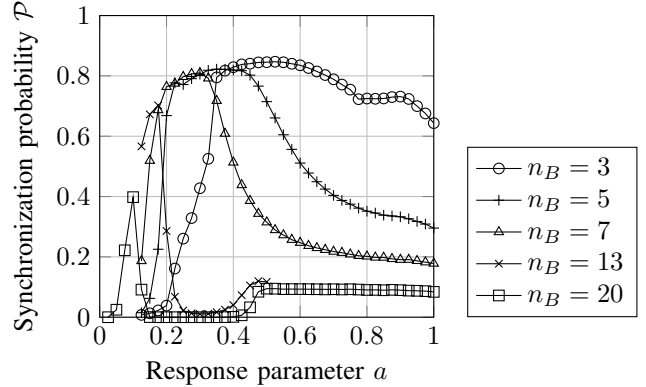


Figure 5. Synchronization probability  $\mathcal{P}$  for  $(10, n_B)$ -diamond bracelets over the response parameter  $a$ . The position and height of the maximum of  $\mathcal{P}$  depends on the size of the diamonds. Values are based on 25,000 simulations using random (uniformly drawn) initial phases.

$\mathcal{P}$  that we already saw for the diamonds is even clearer now and is lower than for a single diamond. Thus, the diamond bracelet lets us more readily identify the maximum values in order to find the optimal  $a$  for which it is achieved, while keeping the basic behavior from the single diamond.

The diamond bracelet allows both types of non-synchronizing states and has a clear optimum of the response parameter, all with only two parameters to control the graph. On this graph, we now study a localized approach to improve the synchronization probability by choosing a node-individual response parameter  $a_i$  for each oscillator  $i$  instead of a single global response parameter  $a$ .

## 5. Local response parameters

Synchronization of diamond bracelets is not always possible. Even an optimal choice of the response parameter  $a$  brings the synchronization probability to a maximum value of only 80–90% (for  $n_B < 7$ ). The synchronization dynamics are governed by the components (ring graphs and  $n_B$ -diamond graphs) that make up the bracelet. We know that these two types of components on their own display optimum  $a$  at different values (see Figs. 3 and 4). It thus stands to reason to try and assign an *individual* response parameter to each oscillator rather than using a global one. In the following, we exemplify that a system with node-individual  $a$  can outperform one with a single, global  $a$  by large in terms of the synchronization probability.

To find a set of  $a$ -values that would improve the synchronization probability achieved by a global  $a$ , we first simplify the problem. There are three types of nodes in the diamond bracelet: ring nodes (index  $R$ ), branch nodes ( $B$ ), and (outer) peak nodes ( $P$ ). Due to network symmetry, we cannot distinguish between any of the diamonds and thus, in an optimal setup and without knowledge of the initial configuration, all ring nodes have the same response parameter  $a_R$ . Likewise, all branch nodes would use  $a_B$  and all peak nodes  $a_P$ . We find optima for these three parameters

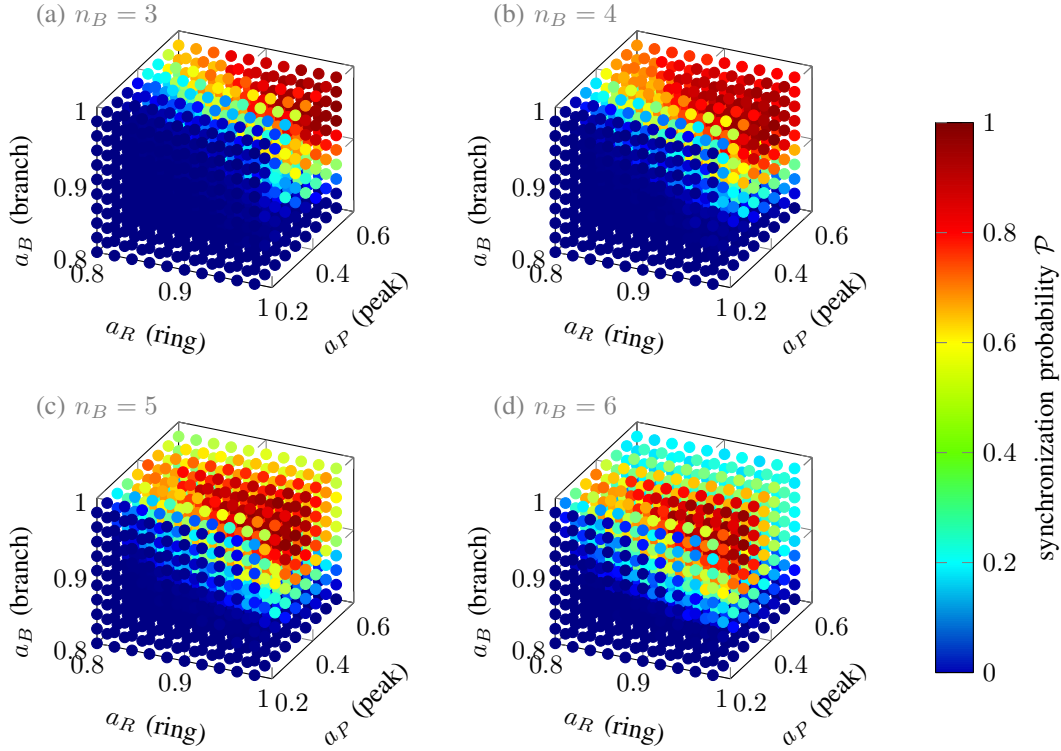


Figure 6. Synchronization probability (color coded) for three independent response parameters  $a_R$  (ring nodes),  $a_B$  (branch nodes), and  $a_P$  (outer peak nodes). Results are shown for a ring with  $n_R = 10$  nodes and four different diamond sizes ( $n_B = 3, \dots, 6$ ). All graphs exhibit the highest synchronization probability for large  $a_R$  and  $a_P$ . The parameter for the branch nodes  $a_B$  achieving the highest synchronization probability decreases with growing  $n_B$ .

by conducting an exhaustive parameter scan. Prior to the results shown, we ran a cursory parameter scan to find the regions of interest. This cursory search suggests large values for  $a_B$  and  $a_R$ , which are least likely to cause deadlocks, and lower values for  $a_P$ , which more easily cause deadlocks at the peak nodes.

Figure 6 shows the synchronization probability  $\mathcal{P}$  for four different  $(10, n_B)$ -bracelets with up to six branch nodes ( $n_B = 3, \dots, 6$ ) as a function of the three response parameters. Empirically, we see: The optimal synchronization probability reaches values above 90% in all these cases. The highest  $\mathcal{P}$  are achieved consistently for large values of  $a_R$  and  $a_B$ . The optimal choice of  $a_P$  depends on  $n_B$  but generally decreases with increasing  $n_B$ . The corresponding curves for global  $a$  are shown for comparison.

As mentioned, the optimal choice for  $a_B$  and  $a_R$  barely depends on the size of the diamonds. The  $a_P$  associated with the highest  $\mathcal{P}$ , however, decreases with  $n_B$ . Intuitively, this may be explained as follows: To synchronize the ring nodes, Section 4.1 tells us that we need a large response parameter. The branch nodes have no risk of running into a deadlock, so  $a_B$  may be chosen very large for a quick synchronization with its neighbors. On the outer peak nodes the degree is  $n_B$ . Since a larger degree increases the risk of deadlocks,  $a_P$  needs to be chosen smaller the larger  $n_B$

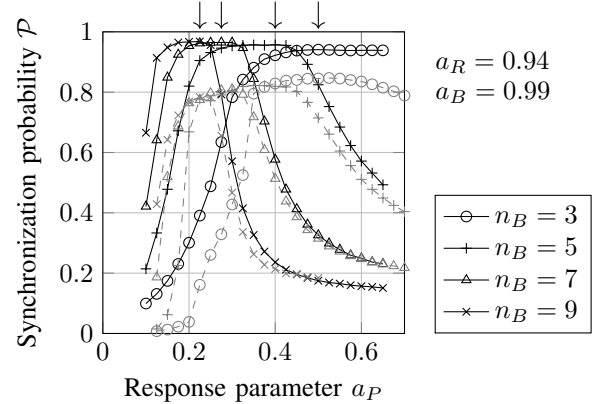


Figure 7. Synchronization probability  $\mathcal{P}$  for several  $n_B$ -diamond bracelets with node-individual response parameters. As motivated by Fig. 6, only the peak node parameter  $a_P$  is varied. The arrows approximately mark the maximum  $\mathcal{P}$ , whose position decreases with  $n_B$ . For reference the plot shows the corresponding  $\mathcal{P}$  curves using global  $a$  in gray. Values are based on 200,000 simulations using random (uniformly drawn) initial phases.

is. Figure 7 shows  $\mathcal{P}$  for several  $(10, n_B)$ -bracelets with  $a_R = 0.94$  and  $a_B = 0.98$  as a function of  $a_P$ . The maximum probabilities are marked in each curve and display the mentioned tendency for the optimal  $a_P$  to shift towards

lower values for increasing  $n_B$ . Due to the flatness of the curves around the maximum, an exact location for the maximum is hard to determine.

Given this exemplary result, it is fair to assume that a localized choice of response parameters has the potential to considerably outperform the global choice not only in diamond bracelets but also in other graphs. We also see that the optimal choice of parameters depends on the topological function of a node. In reality, it is impractical to always scan the entire parameter space (especially when considering that we generally operate with far more dimensions). Developing a distributed algorithm that chooses the  $a$ -value for each node based on local information might be the solution.

## 6. Conclusions and Outlook

It is known that self-organized synchronization via coupling of oscillators cannot always be guaranteed. If the network topology is beyond our control but the individual nodes are not, we can adjust the response parameter to increase the synchronization probability. We demonstrated that diamonds and diamond bracelets, which allow for locked states and deadlocks, have a maximum  $\mathcal{P}$  that depends on network parameters ( $n_B$  and  $n_R$ ). Using node-individual response parameters achieves a larger  $\mathcal{P}$  than using a global one for these topologies. It remains open if suitable response parameters can be calculated using a distributed algorithm, ideally even with only local knowledge. It also remains open if these benefits transfer to other network topologies.

Further research could investigate whether localized response parameters have benefits that go beyond synchronization guarantees. Other performance metrics include synchronization speed as well as robustness against disturbances and dynamic changes of the topology. Furthermore, a combination of localized parameters and stochastic coupling (to prevent deadlocks [17]) could lead to advanced synchronization solutions for self-adaptive networked systems.

## Acknowledgment

This work was partly funded by the Austrian Science Fund (FWF), grant “Self-organizing synchronization with stochastic coupling” (P30012).

## References

- [1] J. Buck and E. Buck, “Biology of Synchronous Flashing of Fireflies,” *Nature*, vol. 211, pp. 562–564, Aug. 1966.
- [2] C. Peskin and Courant Institute of Mathematical Sciences, *Mathematical Aspects of Heart Physiology*. Courant Institute Lecture Notes, Courant Institute of Mathematical Sciences, New York University, 1975.
- [3] P. J. Menck, J. Heitzig, J. Kurths, and H. Joachim Schellnhuber, “How dead ends undermine power grid stability,” *Nature Communications*, vol. 5, p. 3969, June 2014.
- [4] S. H. Strogatz, D. M. Abrams, A. McRobie, B. Eckhardt, and E. Ott, “Crowd synchrony on the Millennium Bridge,” *Nature*, vol. 438, pp. 43–44, Nov. 2005.
- [5] S. Floyd and V. Jacobson, “Random early detection gateways for congestion avoidance,” *IEEE/ACM Transactions on Networking*, vol. 1, pp. 397–413, Aug. 1993.
- [6] C. Hammond, H. Bergman, and P. Brown, “Pathological Synchronization in Parkinson’s Disease: Networks, Models and Treatments,” vol. 30, no. 7, pp. 357–364.
- [7] R. E. Mirollo and S. H. Strogatz, “Synchronization of Pulse-Coupled Biological Oscillators,” *SIAM Journal on Applied Mathematics*, vol. 50, pp. 1645–1662, Dec. 1990.
- [8] S. Marella and G. B. Ermentrout, “Class-II Neurons Display a Higher Degree of Stochastic Synchronization Than Class-I Neurons,” *Physical Review E*, vol. 77, p. 041918, Apr. 2008.
- [9] A. Abouzeid and B. Ermentrout, “Type-II Phase Resetting Curve is Optimal for Stochastic Synchrony,” *Physical Review E*, vol. 80, p. 011911, July 2009.
- [10] Y. Wang and F. J. Doyle III, “Optimal Phase Response Functions for Fast Pulse-Coupled Synchronization in Wireless Sensor Networks,” *IEEE Transactions on Signal Processing*, vol. 60, pp. 5583–5588, Oct. 2012.
- [11] U. Ernst, K. Pawelzik, and T. Geisel, “Delay-induced Multistable Synchronization of Biological Oscillators,” *Physical Review E*, vol. 57, pp. 2150–2162, Feb. 1998.
- [12] P. Bressloff and S. Coombes, “Symmetry and Phase-locking in a Ring of Pulse-Coupled Oscillators with Distributed Delays,” *Physica D: Nonlinear Phenomena*, vol. 126, pp. 99–122, Feb. 1999.
- [13] P. C. Bressloff, S. Coombes, and B. de Souza, “Dynamics of a Ring of Pulse-Coupled Oscillators: Group-Theoretic Approach,” *Physical Review Letters*, vol. 79, pp. 2791–2794, Oct. 1997.
- [14] M. Timme, F. Wolf, and T. Geisel, “Topological Speed Limits to Network Synchronization,” *Physical Review Letters*, vol. 92, p. 074101, Feb. 2004.
- [15] F. Núñez, Y. Wang, and F. J. Doyle, “Global Synchronization of Pulse-Coupled Oscillators Interacting on Cycle Graphs,” *Automatica*, vol. 52, pp. 202–209, Feb. 2015.
- [16] H. Lyu, “Global Synchronization of Pulse-Coupled Oscillators on Trees,” *SIAM Journal on Applied Dynamical Systems*, vol. 17, pp. 1521–1559, Jan. 2018.
- [17] J. Klinglmayr, C. Kirst, C. Bettstetter, and M. Timme, “Guaranteeing Global Synchronization in Networks With Stochastic Interactions,” *New Journal of Physics*, vol. 14, p. 073031, July 2012.
- [18] Y. Wang, F. Nunez, and F. J. Doyle, “Increasing Sync Rate of Pulse-Coupled Oscillators via Phase Response Function Design: Theory and Application to Wireless Networks,” *IEEE Transactions on Control Systems Technology*, vol. 21, pp. 1455–1462, July 2013.
- [19] M. Timme, F. Wolf, and T. Geisel, “Coexistence of Regular and Irregular Dynamics in Complex Networks of Pulse-Coupled Oscillators,” *Physical Review Letters*, vol. 89, p. 258701, Nov. 2002.
- [20] A. Vogell, U. Schilcher, and C. Bettstetter, “Deadlocks in the Synchronization of Pulse-Coupled Oscillators on Star Graphs,” *Physical Review E*, vol. 102, p. 062211, Dec. 2020.
- [21] C. v. Vreeswijk and H. Sompolinsky, “Chaos in Neuronal Networks with Balanced Excitatory and Inhibitory Activity,” *Science*, vol. 274, pp. 1724–1726, Dec. 1996.
- [22] M. Timme, F. Wolf, and T. Geisel, “Unstable Attractors Induce Perpetual Synchronization and Desynchronization,” *Chaos: An Interdisciplinary Journal of Nonlinear Science*, vol. 13, pp. 377–387, Mar. 2003.
- [23] S. Olmi, A. Politi, and A. Torcini, “Collective Chaos in Pulse-Coupled Neural Networks,” *Europhysics Letters*, vol. 92, p. 60007, Dec. 2010.